

# A label-free immunosensor for detecting common acute lymphoblastic leukemia antigen (CD10) based on gold nanoparticles by quartz crystal microbalance

Zhiyong Yan, Min Yang, Zonghua Wang\*, Feifei Zhang, Jianfei Xia, Guoyu Shi, Lin Xia, Yanhui Li, Yanzhi Xia, Linhua Xia

*Collaborative Innovation Center for Marine Biomass Fiber Materials and Textiles, College of Chemical Science and Engineering, Shandong Sino-Japanese Center for Collaborative Research of Carbon Nanomaterials, Laboratory of Fiber Materials and Modern Textiles, the Growing Base for State Key Laboratory, Qingdao University, Qingdao, Shandong 266071, China*

## ARTICLE INFO

### Article history:

Received 2 July 2014

Received in revised form

12 December 2014

Accepted 26 December 2014

Available online 3 January 2015

### Keywords:

CD10

QCM

Label-free

Immunosensor

Au NPs

## ABSTRACT

Rapid and sensitive detection of the common acute lymphoblastic leukemia antigen (CD10) is crucial for diagnosing and prognosing hematopoietic tumors and several carcinomas. In the present study, a label-free immunosensor for detecting CD10 by Quartz Crystal Microbalance (QCM) was developed. The detection system has a good selectivity based on the biospecific interactions between the CD10 antigen and antibody, and the sensitivity of the immunosensor was further improved for Au NPs not only carried more antibodies but also acted as mass enhancers. Experimental results confirmed that this developed method could be conveniently used for the detection of CD10 without labeling, and CD10 could be measured quantitatively in the concentration range from  $1.0 \times 10^{-8}$  to  $1.0 \times 10^{-11}$  M.

© 2015 Elsevier B.V. All rights reserved.

## 1. Introduction

Common acute lymphoblastic leukemia antigen, known as CD10, is a zinc-dependent metalloendoprotease. It plays important roles as a multifaceted environment actor in stem cells, physiological mechanisms and cancer [1]. CD10 was first identified in leukemia as tumor-specific antigen for it expresses in acute lymphoblastic leukaemia and follicle center cell lymphoma [2], then it has been widely used for evaluating tumor progression [3]. Deregulation of CD10 expression may cause severe disturbances in cells and their environment, ultimately lead to serious diseases. Therefore, sensitive and accurate detection of CD10 is indispensable.

Previous studies of CD10 usually paid more attention on the biologic role of CD10 rather than the quantitative analysis of CD10 [4,5]. In order to quantitative detect CD10, our group has developed an electrochemical immunosensor by using scanning electrochemical microscopy [6]. Reduction current which reflected the concentration of CD10 was monitored and a current

topographic image corresponded to the specific binding between CD10 and anti-CD10 was also provided. Though sensitive detection of CD10 was achieved with a detection limit of  $4.38 \times 10^{-12}$  M, the signal was inevitably to be interrupted because the binding reaction was detected indirectly. In order to quantitative analysis CD10 in a straightforward way, herein, a label-free immunosensor for detecting CD10 based on Au NPs by QCM is reported.

QCM is an efficient mass detection instrument [7]. After the analyte is captured on the quartz crystal, the frequency shift reflects the corresponding mass change, thus offering the reaction information in real time. Compared with the traditional antigen detection methods (chemiluminescence detection [8], fluorescence detection [9], electrochemical methods [10], etc.) which are usually recognized through the signals generated from labels such as enzymes [11], radioactive isotopes [12] or fluorescent agents [13], QCM can detect the physical and chemical changes of antigen–antibody reaction directly while preventing the interference. Moreover, the detection process is less sophisticated in contrast with other label-free methods such as immunosensor based on surface plasmon resonance [14]. Thus QCM becomes attractive tool and has gained considerable interest. In previous reports, QCM has been successfully used in gel spreading [15], gas adsorption [16], biomolecule detection (such as DNA [17], enzyme [18], liposome [19]), etc. QCM

\* Corresponding author. Tel.: +86 0532 85950873; fax: +86 0532 85950873.

E-mail addresses: [wangzonghua@qdu.edu.cn](mailto:wangzonghua@qdu.edu.cn), [13853219173@126.com](mailto:13853219173@126.com) (Z. Wang).

has also been utilized in immunoassays. For instance, Shons et al. used QCM to determine the antibody activity [20]. Since then relevant studies have been subsequently reported, referring to the use of QCM for the detection of antigen–antibody reaction. Kyusik et al. [21] utilized QCM to analyze the binding of immunoliposomes with antigen, and investigated the action of liposomes as the signal enhancing reagents in competitive QCM immunoassay. Wang et al. has developed an integrated QCM immunosensor array to explore the differentiated leukocyte antigens for immunophenotyping of acute leukemia [22].

Because the mass change from the binding of antigen on the crystal surface is small, it is necessary to further improve sensitivity of QCM immunosensor. Many signal enhancers have been used in QCM sensors such as nanoparticles, enzymes, liposomes, etc. Among them, nanoparticles demonstrate a great potential in increasing sensitivity, for they have a relatively large mass compared to most analytes and the ability to be surface functionalized. Generally, Au NPs present good biocompatibility, large specific surface area and high surface free energy, which make them widely used in the field of biological chemistry [23–26]. Au NPs have generated an increasing attention serving as excellent carriers for the loading of signal tags, such as proteins [27,28], quantum dots [29], DNA [30], liposome [31]. Moreover, since Au NPs can change the sensing surface stress obviously, they have also been utilized in mass detection systems such as microcantilever [32] and QCM based platform. Au NPs have been investigated to be utilized in QCM sensors to detect metal ions [33], thrombin [34], bacterial cells [35], etc. However, there are few reports about antigen detection using Au NPs as carriers and mass enhancers in QCM immunosensors.

Herein we utilized Au NPs as signal enhancing reagents with antibody ( $\text{Ab}_2$ ) fixed on their surface, and the resulting composites were bonded specifically to CD10 immobilized on the crystal surface. Due to the mass increase on crystal surface, the frequency change became significantly larger than that without Au NPs. After the layer-by-layer modification of quartz crystal, the mass of the crystal surface increased and the resonance frequency decreased. The shifts of changed frequency correspond to the weight change from the specific attachment of antigens to the antibody immobilized on the quartz crystal surface of QCM. The binding information of antigen and antibody without any labels can be achieved in real time.

## 2. Materials and methods

### 2.1. Materials

CD10 and CD10 antibody (Ab) were purchased from Biosynthesis Biotechnology Co. (Beijing, China). CD10 and Ab were dissolved in phosphate buffered saline (PBS, pH 7.4, containing 0.01 M of phosphate and 0.1 M of KCl), respectively, and stored at 4 °C for subsequent experiments. CD10 solutions with different concentrations were prepared in PBS (pH 7.4).  $\text{HAuCl}_4 \cdot 4\text{H}_2\text{O}$  was purchased from Sinopharm Chemical Reagent Co., Ltd. (Beijing, China). Other chemicals with analytical reagent grade can be directly used as received without any purification. L-Glutathione was purchased from Solarbio. S&T Co. (Beijing, China). In experiments, ultrapure water was used throughout.

### 2.2. Equipments

Q-Sense E1 QCM-D instrument was purchased from Q-Sense AB, Västra Frölunda, Sweden. Gold-coated quartz crystal with a fundamental resonant frequency of 5 MHz was bought from Q-Sense. Morphology and structure of Au NPs were characterized by transmission electron microscopy (TEM; JEOL JEM-2100, operated at

200 kV). Ultraviolet-visible (UV-vis) spectra were recorded on a UV-2800 Ultraviolet spectrophotometer (UNICO Instrument Co., Ltd., Shanghai). Atomic Force Microscopy (AFM) image was taken with a Being Nano-Instruments CSPM-4000 (Benyuan, China).

### 2.3. Fabrication of immunosensor

#### 2.3.1. Preparation of Au NPs

Au NPs were prepared through thermal reduction of  $\text{HAuCl}_4$  by sodium citrate. Firstly, 0.01% of  $\text{HAuCl}_4$  solution and 1.0% of trisodium citrate solution were filtered through 0.22 μm micro-porous membrane filter successively, and then 100 mL of  $\text{HAuCl}_4$  solution (0.01%) was heated until boiling, after that, 3.0 mL of trisodium citrate solution was added. When the color of the solution changed, the following procedures were to stop heating, accompanied by an additional stirring for 15 min. Finally, the resulting Au NPs were stored at 4 °C, and treated with ultrasonic wave before further use.

#### 2.3.2. Preparation of $\text{Ab}_2/\text{Au}$ NPs

To link  $\text{Ab}_2$  to Au NPs and increase the stability at the same time, glutathione was added to Au NPs solution. The resulting mixture was centrifuged for 10 min at 10,000 rpm to remove the excess glutathione. After the achievement of capped Au NPs, freshly prepared EDC solution (5 mM/L) was added to the capped Au NPs with stirring for 15 min to activate the surface carboxylic groups of capped Au NPs. Then, the mixture was centrifuged again and the soft sediment was washed with PBS. After that, 110 μL of  $\text{Ab}_2$  solution ( $1.0 \times 10^{-7}$  M) was added to the capped Au NPs solution to form the mixture at 4 °C for 9 h. Subsequently,  $\text{Ab}_2$  was modified on the capped Au NPs by forming an amide bond between the carboxylic group and amino group. After the centrifugation and discard of supernatants, the resulting  $\text{Ab}_2/\text{Au}$  NPs were finally re-dispersed in PBS (pH 7.4), and stored at 4 °C for further use.

### 2.4. QCM measurement procedure

Before a particular use, the quartz crystal of QCM needs to be cleaned with piranha solution, followed by the treatment of a 3:1 (volume ratio) mixture of concentrated sulfuric acid and hydrogen peroxide, and the rinse with deionized water. Afterward, the treated quartz crystal was immersed in a boiling mixture ( $V_{\text{ultrapure water}}:V_{\text{ammonia}}:V_{\text{hydrogen peroxide}} = 5:1:1$ ) for 10–15 min. Finally, the quartz crystal was cleaned with ultrapure water, and then blew with a stream of dry nitrogen gas. Before the quartz crystal was put on reaction cell, relevant important procedures should be performed, including the treatment of the gold surface of quartz crystal with 15 μL of MPA (3-mercaptopropionic acid, 10 mM) overnight, the activation with the EDC/NHS solution for an hour to produce the carboxyl quartz crystal, and the washing treatment of the quartz crystal with PBS.

The schematic representations of CD10 detection by QCM and a typical QCM readout for CD10 detection procedure were exhibited in Figs. 1 and 2, respectively. The figures showed the binding of  $\text{Ab}_2/\text{Au}$  NPs to CD10 immobilized with  $\text{Ab}_1$  on the gold coated crystal surface, and the morphology was characterized by AFM shown in Fig. S1 (see Supplementary materials). The numerous “islands” in the image above clearly showed the binding of  $\text{Ab}_2/\text{Au}$  NPs to CD10 immobilized with  $\text{Ab}_1$  on the gold coated crystal surface. After PBS was pumped into the cell at a flow rate of 60 μL/min, the quartz crystal was put into the cell. When the frequency got stable,  $1.0 \times 10^{-7}$  M of  $\text{Ab}_1$  was added and incubated for an hour, which helped to its cross-linking on the activated gold surface via its N-terminal amino group. After that, the stable frequency (F1) of the quartz crystal immobilized with  $\text{Ab}_1$  was recorded. In PBS, CD10 solutions with different concentrations from  $1.0 \times 10^{-8}$  M to

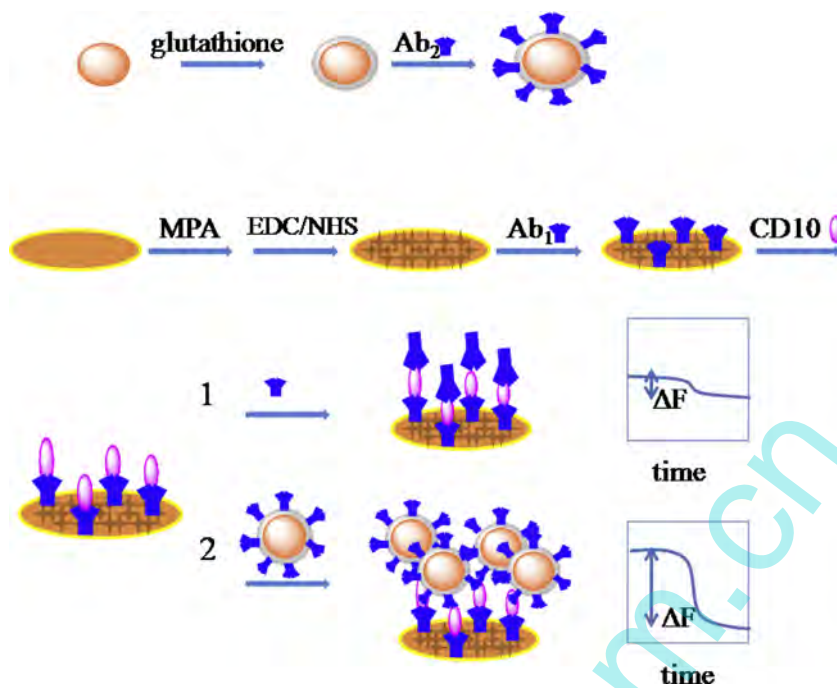


**Fig. 1.** Schematic representation of CD10 detection by QCM.

$1.0 \times 10^{-11}$  M were pumped into the cell, and incubated for an hour. Finally,  $\text{Ab}_2/\text{Au}$  NPs in PBS was added and immobilized on the  $\text{CD}10/\text{Ab}_1$  quartz crystal for reaction. After reaction, PBS solution was injected to wash the nonspecific bound  $\text{Ab}_2$ , and the stable frequency  $F_2$  was recorded again. The frequency change ( $\Delta F = F_2 - F_1$ ) was related to the total amount of  $\text{CD}10$  immobilized with  $\text{Ab}_1$  on the quartz crystal. At the same concentration, the frequency changes of  $\text{Ab}_2/\text{Au}$  NPs and  $\text{Ab}_2$  (Fig. 2A and B) were compared. When the  $\text{Ab}_2/\text{Au}$  NPs was used, the frequency change was much bigger than that when only the  $\text{Ab}_2$  was used. Upon reaching 100 Hz, the stable frequency between  $\text{CD}10$  and  $\text{Ab}_2/\text{Au}$  NPs was 40 Hz. When the  $\text{Ab}_2$  was used alone, the frequency change was close to 60 Hz, while the stable frequency change between  $\text{CD}10$  and  $\text{Ab}_2$  was approximately 10 Hz. The probably reason is that Au NPs carry more  $\text{Ab}_2$ , allowing specific binding to more  $\text{CD}10$ . Moreover, the Au NPs modified with  $\text{Ab}_2$  were adsorbed on the crystal, thus inducing the increase of the crystal surface mass and the decrease of the resonance frequency.

### 3. Results and discussion

#### 3.1. Characterization and modification of Au NPs

Morphology and structure of Au NPs were characterized by TEM. The prepared Au NPs have an average diameter of 15–18 nm (Fig. 3A), indicating a regular shape. The Au NPs were also characterized by UV-visible absorption spectrum, and the maximum absorption peak was around 520 nm (Fig. 3B). The Au NPs used in our study were synthesized by the reduction of an aurate salt with reducing agents. Thus they need to be surface modified to be more stable and compatible for preparation of bioconjugate in the subsequent experience. Amino ( $-\text{NH}_2$ ) and thiol ( $-\text{SH}$ ) groups are known to have high affinity for the gold. There are two carboxylic groups, one thiol group and three amino groups in glutathione [36], thus glutathione was chosen as capping agents to protect the Au NPs from clustering. At the same time,  $\text{Ab}_2$  can be linked on the Au NPs by an amide bond formed between the carboxylic groups of

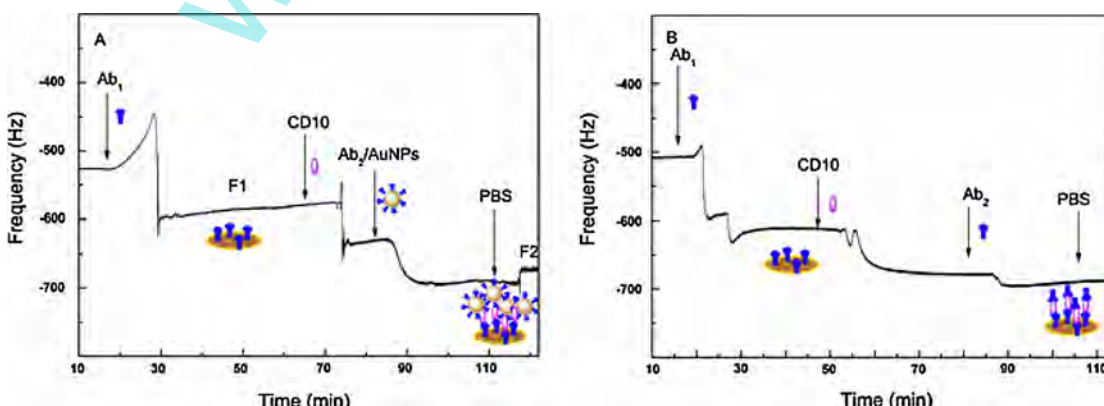


**Fig. 2.** (A) A typical QCM readout of the  $\text{CD}10$  detection procedure; (B) QCM readout without Au NPs.

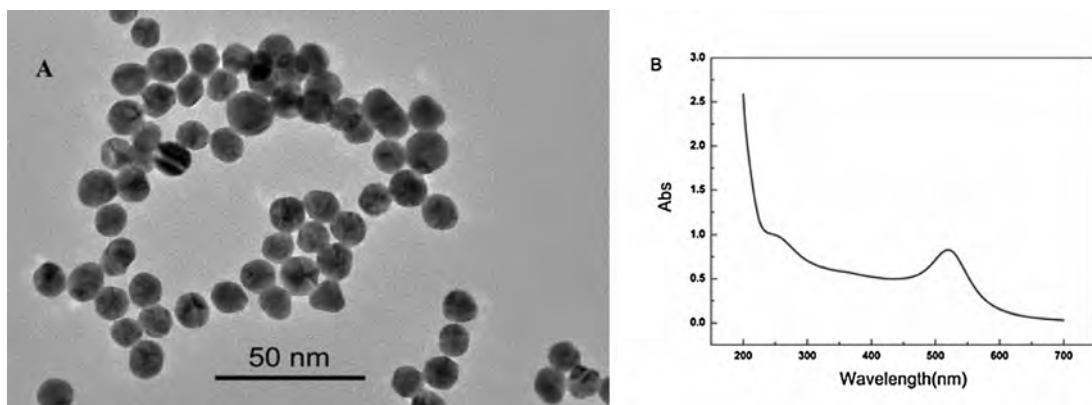


**Fig. 3.** (A) TEM image of Au NPs; (B) the UV-visible spectrum of Au NPs.

glutathione capped Au NPs and amino groups present in the Ab<sub>2</sub> antibody, come into being a sandwich-type structure on the surface of quartz crystal.

### 3.2. Preparation of the immunosensor

The schematic representations of preparation processes of the immunosensor and the detection strategy were shown in Fig. 1. After a sandwich-type immunoreaction, the CD10 antigen and Ab<sub>2</sub>/Au NPs were captured on the surface of quartz crystal, and the frequency change reflected the immunoreactions.

### 3.3. Optimization of detection conditions

In this developed sensing platform, the concentration of Ab<sub>1</sub> is a crucial component. A high Ab<sub>1</sub> concentration may increase the steric hindrance, which is unfavorable for the specific binding with CD10. However, a low Ab<sub>1</sub> concentration may affect the binding efficiency with CD10. To measure the response as a function of the Ab<sub>1</sub> concentration of the immunosensor, different amounts of Ab<sub>1</sub> assays were conducted. When a series of Ab<sub>1</sub> samples with different concentrations from  $1.0 \times 10^{-10}$  M to  $1.0 \times 10^{-6}$  M were used, the frequency changes were markedly different. As exhibited in Fig. 4A, the frequency changes increased with the each increment of Ab<sub>1</sub>.

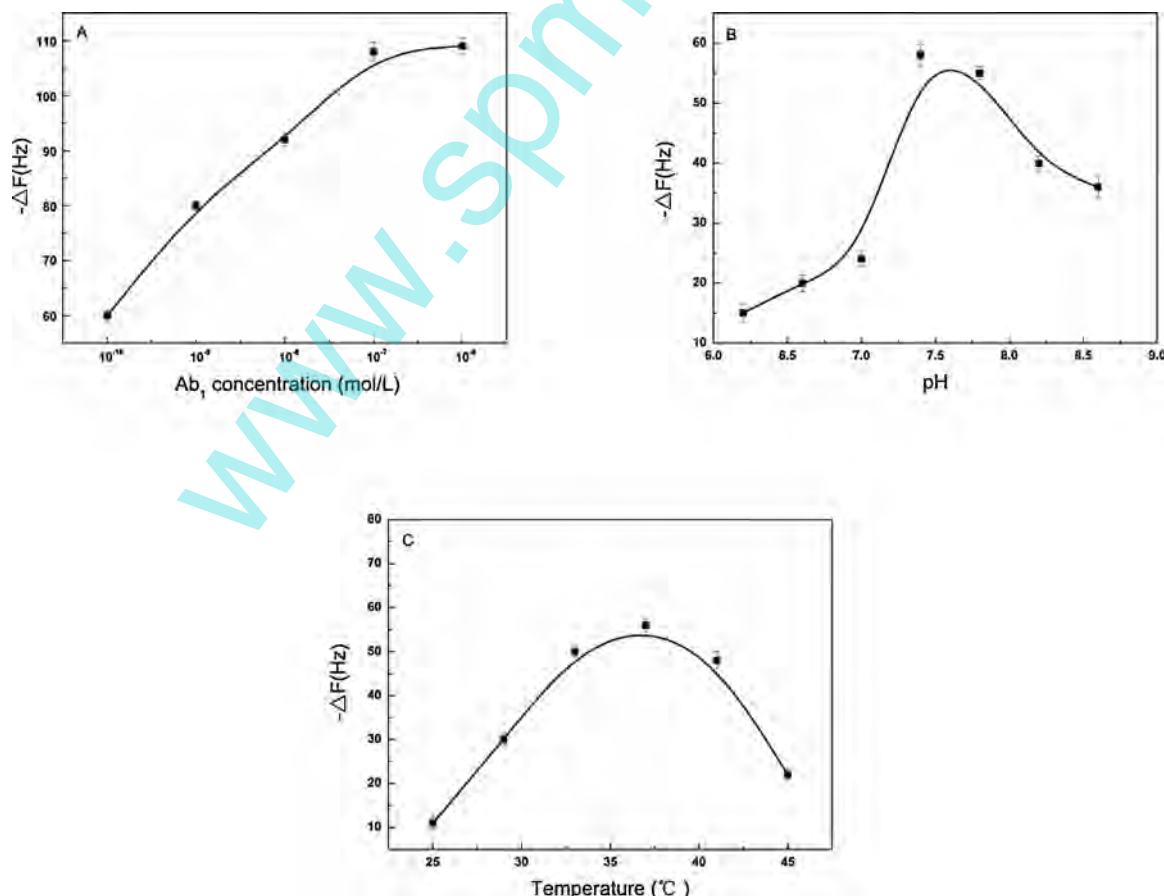


**Fig. 4.** (A) Optimization of the concentration of Ab<sub>1</sub>; (B) optimization of pH; (C) optimization of the temperature.

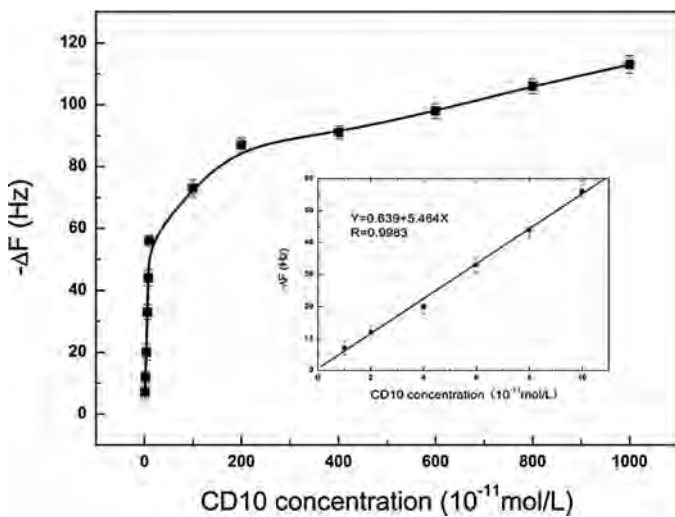


**Fig. 5.** Real-time frequency responses of QCM immunosensor for detection of CD10. The concentrations of CD10 were from  $1.0 \times 10^{-8}$  to  $1.0 \times 10^{-11}$  M. The insert shows linear relationship between the frequency shifts and the concentration of CD10 antigen in the range from  $1.0 \times 10^{-11}$  M to  $1.0 \times 10^{-10}$  M. Error bars are standard deviation of three repetitive measurements.

amount. Especially, a sufficient frequency change could be obtained at  $1.0 \times 10^{-7}$  M, which was thus used for following experiments.

The performance of this immunosensor was depended on the pH and temperature. As shown in Fig. 4B, the maximum response from pH appeared at pH 7.4, which was thus selected in this study. As demonstrated in Fig. 4C, the optimal temperature was 37 °C.

#### 3.4. QCM detection of the immunosensor

Under the optimized assay conditions, a series of antigens in the concentration range from  $1.0 \times 10^{-8}$  M to  $1.0 \times 10^{-11}$  M were determined, as shown in Fig. 5. The QCM is a piezoelectric sensor and its resonant frequency ( $\Delta F$ ) is proportional to changes in mass adsorbed on the quartz surface under certain conditions according to the Sauerbrey equation:  $\Delta F = -C_f \Delta m$ , in which  $C_f$  is a constant dependent on the quartz properties [37]. Therein, the frequency shifts of Ab<sub>2</sub>/Au NPs were in response to the CD10 of different concentrations. With the increase of CD10 concentration, the CD10 frequency change increased, indicating that the more CD10 was specifically bonded with antibody. In addition, the frequency shift has a good linear relationship with the concentration of CD10 in the range from  $1.0 \times 10^{-11}$  M to  $1.0 \times 10^{-10}$  M. The detection limit is  $2.4 \times 10^{-12}$  M (3σ method,  $n = 11$ ). When the concentration of CD10 continued to increase, the chemical absorption on the quartz crystal tended to saturation gradually, and finally the adsorption phase achieved the saturation limit of the surface coverage.

The results from relevant experiments performed without CD10 were shown in Fig. S2 (see Supplementary materials). As observed, after PBS was pumped in the detection cell to wash the nonspecifically bonding Ab<sub>2</sub>/Au NPs, the frequency change was rather small and even could be ignored, which may be ascribed to the absence of CD10. On this account, none of Ab<sub>2</sub>/Au NPs was modified on the quartz crystal, and thus the frequency could not be changed.

#### 3.5. Specificity and repeatability of the immunosensor

Specificity of the detection was evaluated by testing response of other human lymphocyte antigens (CD19 and CD20). Higher shift of frequency was observed with the CD10 than CD19 and CD20 (Fig. 6). When mixed with these three antigens, the frequency shift had no obvious change compared with that of CD10. These results clearly

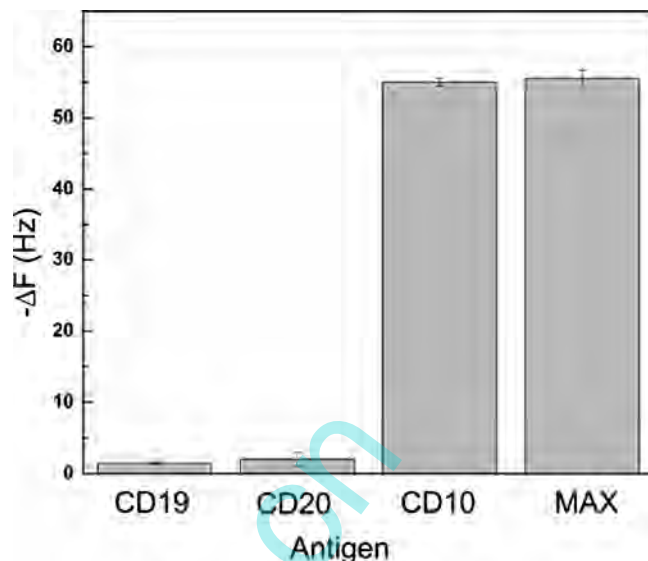


**Fig. 6.** Frequency responses after the addition of CD10, CD19 and CD20. The concentration of CD10:  $1.0 \times 10^{-10}$  M. The concentration of CD19 and CD20:  $1.0 \times 10^{-8}$  M.

demonstrated that the non-target molecules did not interfere with the CD10 analysis and this method has good specificity for the CD10 antigen. The repeatability of the immunosensor was estimated by the measurement the frequent change of the immunoassays which were fabricated on the same surface of quartz crystal and used the same suspension of Ab<sub>2</sub>/Au NPs under the optimized experiment conditions for six times. The corresponding results showed an acceptable repeatability with a relative standard deviation (RSD) of 5.8%.

#### 4. Conclusions

In this work, a label-free sandwich immunosensing method was reported to detect the CD10 antigen by using QCM. Au NPs worked as the antibody carriers and mass signal enhancers. According to the frequency change, the immune response process of CD10 and anti-CD10 could be detected in real time. Furthermore, the procedure was simple and easy to be operated. This label-free sandwich immunosensing method could detect the CD10 concentration in the range from  $1.0 \times 10^{-8}$  to  $1.0 \times 10^{-11}$  M. We expect this platform to be developed into a promising application in real sample analysis.

#### Acknowledgments

We greatly appreciate the financial support from the National Natural Science Foundation of China (21475071, 21405086, 21275082, 21203228 and 81102411), the National Key Basic Research Development Program of China (973 special preliminary study plan, Grant no.: 2012CB722705), the Taishan Scholar Program of Shandong Province and the Natural Science Foundation of Qingdao (13-1-4-128-jch and 13-1-4-202-jch).

#### Appendix A. Supplementary data

Supplementary data associated with this article can be found, in the online version, at <http://dx.doi.org/10.1016/j.snb.2014.12.104>.

#### References

- [1] V. Maguer-Satta, R. Besancon, E. Bachelard-Cascales, Concise review: neutral endopeptidase (CD10): a multifaceted environment actor in stem cells, physiological mechanisms, and cancer, *Stem Cells* 29 (2011) 389–396.

- [2] W.G. McCluggage, V.P. Sumathi, P. Maxwell, CD10 is a sensitive and diagnostically useful immunohistochemical marker of normal endometrial stroma and of endometrial stromal neoplasms, *Histopathology* 39 (2001) 273–278.
- [3] P.G. Chu, D.A. Arber, L.M. Weiss, K.L. Chang, Utility of CD10 in distinguishing between endometrial stromal sarcoma and uterine smooth muscle tumors: an immunohistochemical comparison of 34 cases, *Mod. Pathol.* 14 (2001) 465–471.
- [4] P.E. Milhiet, F. Dennin, M.C. Giocondi, C.L. Grimalle, C. Garbay-Jaureguiberry, C. Boucheix, B.P. Roques, Detection of neutral endopeptidase-24.11/CD10 by flow cytometry and photomicroscopy using a new fluorescent inhibitor, *Anal. Biochem.* 205 (1992) 57–64.
- [5] A. Stacchini, A. Demurtas, S. Aliberti, P.F. Celle, L. Godio, G. Palestro, D. Novero, The usefulness of flow cytometric CD10 detection in the differential diagnosis of peripheral T-cell lymphomas, *Am. J. Clin. Pathol.* 128 (2007) 854–864.
- [6] W.L. Song, Z.Y. Yan, K.C. Hu, Electrochemical immunoassay for CD10 antigen using scanning electrochemical microscopy, *Biosens. Bioelectron.* 38 (2012) 425–429.
- [7] A.A. Suleiman, G.G. Guilbault, Recent developments in piezoelectric immunosensors, *Analyst* 119 (1994) 2279–2282.
- [8] C. Zong, J. Wu, C. Wang, H.X. Ju, F. Yan, Chemiluminescence imaging immunoassay of multiple tumor markers for cancer screening, *Anal. Chem.* 84 (2012) 2410–2415.
- [9] N. Li, A.M. Chow, H.V.S. Ganesh, I.R. Brown, K. Kerman, Quantum dot based fluorometric detection of cancer TF-antigen, *Anal. Chem.* 85 (2013) 9699–9704.
- [10] J. Zhou, L.P. Du, L. Zou, Y.C. Zou, N. Hu, P. Wang, An ultrasensitive electrochemical immunosensor for carcinoembryonic antigen detection based on staphylococcal protein A-Au nanoparticle modified gold electrode, *Sens. Actuators, B* 197 (2014) 220–227.
- [11] J.L. Zhang, X. Chen, M.H. Yang, Enzyme modified peptide nanowire as label for the fabrication of electrochemical immunosensor, *Sens. Actuators, B* 196 (2014) 189–193.
- [12] M. Andratschke, C.W. Luebbers, V. Johannson, B. Schmitt, B. Mack, R. Zeidler, S. Lang, B. Wollenberg, F.J. Gildehaus, Biodistribution of 131I-labeled anti-CK8 monoclonal antibody in HNSCC in xenotransplanted SCID mice, *Cancer Res.* 31 (2011) 3315–3321.
- [13] Y.D. Zhu, J. Peng, L.P. Jiang, J.J. Zhu, Fluorescent immunosensor based on CuS nanoparticles for sensitive detection of cancer biomarker, *Analyst* 139 (2013) 649–655.
- [14] C. Boozer, G. Kim, S. Cong, H.W. Guan, T. Lonergan, Looking towards label-free biomolecular interaction analysis in a high-throughput format: a review of new surface plasmon resonance technologies, *Curr. Opin. Biotechnol.* 17 (2006) 400–405.
- [15] F.N. Nunalee, K.R. Shull, QCM studies of gel spreading: kraton gels on polystyrene surfaces, *Langmuir* 22 (2006) 431–439.
- [16] Y.T. Wu, P.J. Akoto-Ampaw, M. Elbaccouch, M.L. Hurrey, S.L. Wallen, C.S. Grant, Quartz crystal microbalance (QCM) in high-pressure carbon dioxide (CO<sub>2</sub>): experimental aspects of QCM theory and CO<sub>2</sub> adsorption, *Langmuir* 20 (2004) 3665–3673.
- [17] R.J. Rawle, M.S. Johal, C.R.D. Selassie, A real-time QCM-D approach to monitoring mammalian DNA damage using DNA adsorbed to a polyelectrolyte surface, *Biomacromolecules* 9 (2008) 9–12.
- [18] G. Graf, V. Kocherbitov, Determination of sorption isotherm and rheological properties of lysozyme using a high-resolution humidity scanning QCM-D technique, *J. Phys. Chem. B* 117 (2013) 10017–10026.
- [19] H. Brochu, P. Vermette, Liposome layers characterized by quartz crystal microbalance measurements and multilayer release delivery, *Langmuir* 23 (2007) 7679–7686.
- [20] A. Shons, F. Dorman, J. Najarian, An immunospecific microbalance, *J. Biomed. Mater. Res.* 6 (1972) 565–570.
- [21] K. Yun, E. Kobatake, T. Haruyama, M.L. Laukkonen, K. Keinänen, M. Aizawa, Use of a quartz crystal microbalance to monitor immunoliposome-antigen interaction, *Anal. Chem.* 70 (1998) 260–264.
- [22] H. Wang, H. Zeng, Z.M. Liu, Y.H. Yang, T. Deng, G.L. Shen, R.Q. Yu, Immunophenotyping of acute leukemia using an integrated piezoelectric immunosensor array, *Anal. Chem.* 76 (2004) 2203–2209.
- [23] R.N. Goyal, M.A. Aziz, M. Oyama, S. Chatterjee, A.R.S. Rana, Nanogold based electrochemical sensor for determination of norepinephrine in biological fluids, *Sens. Actuators, B* 153 (2011) 232–238.
- [24] S.J. Xu, Y. Liu, T.H. Wang, J.H. Li, Positive potential operation of a cathodic electrogenerated chemiluminescence immunosensor based on luminol and graphene for cancer biomarker detection, *Anal. Chem.* 83 (2011) 3817–3823.
- [25] S.J. Xu, Y. Liu, T.H. Wang, J.H. Li, Highly sensitive electrogenerated chemiluminescence biosensor in profiling protein kinase activity and inhibition using gold nanoparticle as signal transduction probes, *Anal. Chem.* 82 (2010) 9566–9572.
- [26] Y.Z. Wang, Z.H. Chen, Y. Liu, J.H. Li, A functional glycoprotein competitive recognition and signal amplification strategy for carbohydrate-protein interaction profiling and cell surface carbohydrate expression evaluation, *Nanoscale* 5 (2013) 7349–7355.
- [27] Y. Liu, Y. Liu, R.L. Mernaugh, X.Q. Zeng, Single chain fragment variable recombinant antibody functionalized gold nanoparticles for a highly sensitive colorimetric immunoassay, *Biosens. Bioelectron.* 24 (2009) 2853–2857.
- [28] X.J. Chen, Y.Z. Wang, Y.Y. Zhang, Z.H. Chen, Y. Liu, Z.L. Li, J.H. Li, Sensitive electrochemical aptamer biosensor for dynamic cell surface N-glycan evaluation featuring multivalent recognition and signal amplification on a dendrimer-graphene electrode interface, *Anal. Chem.* 86 (2014) 4278–4286.
- [29] O. Kulakovitch, N. Strekal, A. Yaroshevich, S. Maskevich, S. Gaponenko, I. Nabiev, U. Woggon, M. Artemyev, Enhanced luminescence of CdSe quantum dots on gold colloids, *Nano Lett.* 2 (2002) 1449–1452.
- [30] Z.H. Wang, N. Sun, Y. He, Y. Liu, J.H. Li, DNA assembled gold nanoparticles polymeric network blocks modular highly sensitive electrochemical biosensors for protein kinase activity analysis and inhibition, *Anal. Chem.* 86 (2014) 6153–6159.
- [31] X.Q. An, F. Zhang, Y.Y. Zhu, W.G. Shen, Photoinduced drug release from thermosensitive Au NPs-liposome using a Au NPs-switch, *Chem. Commun.* 46 (2010) 7202–7204.
- [32] M. Alvarez, L.M. Lechuga, Microcantilever-based platforms as biosensing tools, *Analyst* 135 (2010) 827–836.
- [33] H.B. Teh, H. Li, S.F.Y. Li, Highly sensitive and selective detection of Pb<sup>2+</sup> ion using a novel and simple DNAzyme-based quartzcrystal microbalance with dissipation biosensor, *Analyst* 139 (2014) 5170–5175.
- [34] Q. Chen, W. Tang, D.Z. Wang, X.J. Wu, N. Li, F. Liu, Amplified QCM-D biosensor for protein based on aptamer-functionalized gold nanoparticles, *Biosens. Bioelectron.* 26 (2010) 575–579.
- [35] X. Guo, C.S. Lin, S.H. Chen, R. Ye, V.C.H. Wu, A piezoelectric immunosensor for specific capture and enrichment of viable pathogens by quartz crystal microbalance sensor, followed by detection with antibody-functionalized gold nanoparticles, *Biosens. Bioelectron.* 38 (2012) 177–183.
- [36] G.K. Ahirwal, C.K. Mitra, Direct electrochemistry of horseradish peroxidase-gold nanoparticles conjugate, *Sensors* 9 (2009) 881–894.
- [37] G. Sauerbrey, The use of quartz oscillators for weighing thin layers and for microweighting, *Z. Z. Phys.* 155 (1959) 206–222.

## Biographies

**Zhiyong Yan** is a doctoral student. Her research focuses on nanomaterials and biosensors.

**Min Yang** is a lecturer. Her research focuses on chemistry.

**Zonghua Wang** is a professor. Her research focuses on nanomaterials and the biosensors.

**Feifei Zhang** is a lecturer. Her research focuses on electro-analytical chemistry.

**Jianfei Xia** is an associate professor. His research focuses on analytical chemistry.

**Guoyu Shi** is a graduate student. His research focuses on catalyst for fuel cells.

**Lin Xia**, a Ph.D. His research focuses on nano optoelectronic devices.

**Yanhui Li** is a professor. His research focuses on carbon nanotubes.

**Yanzhi Xia** is a professor. His research focuses on fiber materials and modern textile.

**Linhua Xia** is a professor. His research focuses on the materials.